Research on tubular joints at Nanyang Technological University

Lie, S. T.; Chiew, Sing Ping; Lee, Chi King

2009

Chiew, S. P., Lee, C. K., & Lie, S. T. (2009). Research on tubular joints at Nanyang Technological University. The IES Journal Part A: Civil & Structural Engineering, 2(1), 68-84.

https://hdl.handle.net/10356/102891

https://doi.org/10.1080/19373260802582675

TECHNICAL PAPER

Research on tubular joints at Nanyang Technological University

S. P. Chiew, C. K. Lee and S. T. Lie

School of Civil and Environmental Engineering
Nanyang Technological University, 50 Nanyang Avenue, Singapore 639798

(*Received 26 September 2008; final version 24 October 2008*)
Pre-printed version of the paper published in the journal: IES Journal Part A, Vol. 2 pp68-84, 2009

Presented herein is a review of the research programmes and findings on the fatigue performances of tubular joints. The studies, conducted at the Nanyang Technological University, embraced a number of welded tubular joints types that have been used in both onshore and offshore structures. Research efforts also focussed on the development of research methodologies, new modelling and assessment tools that are applicable to different types of commonly used tubular joints. Based on the key results obtained from the studies, those parameters that critically affect the fatigue performance of tubular joints are identified. In addition, some potential areas for further extensions of the presented works are suggested.

Keywords: welded tubular joints, fatigue assessment, numerical modelling, full scale experiment studies

1. Introduction

In the design of tubular steel structures, the importance of the fatigue performance on safety was well appreciated as evidenced by the two-part Eurocode 3 (EN 1993, 2004) devoted to specifying the design standard against fatigue and fracture failure. As the design of structural joints is a critical design step for all tubular steel structures (Zhao et al. 2000 and Wardenier 2002), fatigue assessment of welded tubular hollow section joints is one of the most intensively studied topics in tubular joints. Traditionally, studies on the fatigue performance of tubular joints are largely based on the members' geometries (circular hollow section (CHS) or rectangular hollow section (RHS)) and the joint configurations (T/Y/K/N/X joints) used. The reason is that different member geometries and joint configurations affect the stress concentration factor (SCF) and the peak hot spot stress (HSS) along the weld path. These stress concentrations and hot spot stresses eventually determine when and where fatigue cracks are formed and subsequently affect the fatigue life of the joints. In the research of fatigue performance of welded tubular joints, full scale experimental studies are often carried out to understand the performance of joints (Chiew et al. 2004, 2007, Lie et al. 2006b, Lee et al. 2007a). However, since experimental studies are expensive and time consuming to conduct, the alternative methodology of numerical modelling (Chiew et al. 2001, Lie et al. 2004, 2006a, 2006c, Lee et al. 2005, 2007) is commonly employed to complement experimental studies, especially when the responses for a wide range of geometrical parameters are needed. Regarding the procedure for assessing the fatigue performance of a welded joint, two different levels of approaches are possible, namely, (1) the assessment of an intact, uncracked joint using either the *classification method* or the *hot spot stress method* and (2) the assessment of a cracked joint using the *fracture mechanics method* (Zhao et al. 2000). In general, due to the existence of the crack, the assessment of a cracked joint is more complicated than an intact joint and detailed finite element (FE) modelling is almost mandatory.

When the authors' research group started to investigate the fatigue behaviour of tubular joints, it was realized quickly that while different procedures are needed for the modelling of uncracked and cracked joints, the assessment procedures for uncracked and cracked joints should be considered as two parts of *an integrated fatigue assessment scheme* that follows the service life of the joints. Furthermore, consistent numerical modelling procedures should be developed to study the responses of different joint types. This paper reviews the research findings from a series of research projects carried out by the author's research group at the Nanyang Technological University (NTU) over the ten years. Emphases will be given to describe the research methodology adopted, the key research findings discovered and the modelling tools and assessment procedures developed. The layout of the paper is as follows: In the next section, a concise summary on the general research methodology adopted and the

scope of works done will be given. These will be followed by a summary of the modelling and assessment tools developed. Section 4 will be devoted to reporting the key findings. Finally, conclusions of the research studies done and some potential future extensions will be given.

2. Main study procedures and scope of works done

2.1 General requirements

It was realised at the beginning of the research work that the following general requirements are needed for all fatigue studies, regardless of the joint type under consideration:

(1) Fatigue studies on both uncracked and cracked welded joints are needed. In fact, studies on the cracked joints should be regarded as an inevitable follow up assessment for the uncracked joints after they are built and committed for years of services.

(2) To obtain the responses of the joints, full scale tests are the best approach.

(3) Since full scale experimental studies are expensive, any specimen should be fully tested for both uncracked and cracked conditions. In addition, if possible, further fracture and failure tests should be applied to the cracked joint.

(4) Numerical modelling is the only feasible approach to carry out parametric studies in order to investigate the effects of different geometries and loading parameters.

(5) In numerical parametric studies, a large number of models corresponding to different geometrical parameters are to be created. Hence, a consistent geometrical model and an automatic model (FE meshes) creation tool are mandatory to ensure the quality of the modelling results and to allow the parametric study to be completed in a reasonable time.

Based on the above requirements, the whole study procedure for a given joint type was designed to consist of two main components, namely, the *experimental component* and *the numerical component* complementing each another. Figures 1 and 2 show their overall flow charts.

2.2 Experimental component

The experimental component can be further divided into three phases, namely, the *planning phase*, the *testing phase* and the *analysis phase* (Fig. 1). The planning phase involves the selection of section geometry and joint type. Note that the section and joint types eligible for experimental study are largely depended on the capacity and limitations of the equipment available. An appreciation on the constraint of existing equipment is critical during the planning phase (Steps P1 and P2 in Fig. 1). In the construction technology laboratory of NTU, the testing frame available is the 25-tonne multi-axis dynamic testing frame (The “Orange Rig”, Fig. 3). This testing frame was designed to conduct fatigue

simulations for structural joints. It is possible to mount and test T-, Y- and K joints on this rig. The three dynamic actuators mounted on the frame can apply cyclic loadings in three perpendicular (X-Y-Z) axes. The capacities of the actuators are 250kN in the X and Y axes and 100kN in the Z axis and all with a stroke range of ±125 mm. Sophisticated dynamic loading control system is connected to the actuators so that the magnitudes and the frequencies (up to 5Hz) of the cyclic loadings applied by each actuator can be controlled and pre-fixed independently. The maximum capacities of these actuators (250kN and 100kN) allow fatigue tests of full scale tubular joints with section size up to ∅400mm and thickness up to 25mm to be conducted. In the planning phase, the availability of a reasonable preliminary numerical model (Step P4 in Fig. 1) is critical to the design of the test and specimen sizes. A good preliminary numerical model can indicate the position and the stress range of the peak HSS during cyclic loading to avoid yielding. It also allows the researcher to estimate the number of loading cycles needed to fail the specimen.

In the test phase, two compulsory tests, namely, the *static test* and the *fatigue test*, were conducted. The main objective of the static test (Step T2 in Fig. 1) is to study the responses and the characteristics of the uncracked joint under different loading conditions. Hence, extensive strain gauging around the welded joint is needed (Fig. 4). Furthermore, the static test results are employed to validate the correctness of the experimental set up and the accuracy of the FE model constructed based on the pre-test measurement (Step T1). After the static test is completed, fatigue test (Step T3) is conducted by using the three actuators to apply cyclic loading to the specimen. The fatigue test usually needs the longest time to complete as in some cases (Chiew et al. 2007, Lee et al 2007) more than one million loading cycles are needed to fail the joint. To monitor the crack growth rate along the weld profile and the penetration rate through the thickness of the section, the alternating current potential drop (ACPD) technique (Technical Software Consultant Ltd., 1991, Fig. 5) were employed. Normally, due to the constraints of the ACPD equipment, only a portion (e.g. one of the four corners for a RHS joint) of the weld path can be monitored. In this case, the static test and the FE model results are employed to predict the fatigue crack location. The advancement of the fatigue crack is usually scanned for every 200 to 1000 loading cycles and the history of the crack profile is recorded (Fig. 6) until the crack penetrated through the thickness of the affected section. After the fatigue test is completed, if further study on the failure strength of the crack section is required (Lie et al 2006b, 2006c, 2007), the cracked joint could be relocated to another test frame for fracture and failure tests.

After the main test phase is completed, the specimen is opened up along the cracked region (Step A1) for measurement of the length, depth and profile of the final crack for validation against the ACPD results (Step A2). Since one of the main objectives for all fatigue studies is to predict the crack

growth rate, it is essential that in the FE model the shape of the crack surface and front are modelled correctly (Lie et al. 2003, 2005a, Lee et al. 2007). Toward this end, the crack surface shape is measured using a simple clay mould method (Lee et al. 2007, Nguyen 2008) so that the crack surface shape is captured and digitized (Step A3). Finally, in Step A4, the actual crack penetration rate at a given point of the crack can be obtained by processing the ACPD results which recorded the relationship between the crack depth a and the number of loading cycles applied, N. Differentiation of the smoothed data obtained yields the crack growth rate da/dN which can be used with the Paris' law (Paris and Erdogan 1963)

$$\frac{da}{dN} = C(\Delta K)^m \tag{1}$$

for the estimation of the SIF variation along the crack mouth. In Eq. (1), C and m are two material parameters which can be obtained either from the section supplier or from previous studies (Barsom and Novak 1977). ΔK is the range of the SIF in one loading cycle and is equivalent to the maximum SIF value when the minimum loading is set to zero.

2.3 Numerical component

For the numerical component, it can be divided into three phases (Fig. 2) namely, *modelling of uncracked joint* (Steps U1-U4), *modelling of cracked joint* (Steps C1 to C5) and *development of tools and assessment methods* (Steps D1-D4). For both the modelling of uncracked and cracked joints, the procedures employed are similar and involve the following three steps:

(1) Construction of geometrical models to describe the joint geometry and other key details such as the weld profile, shapes of crack surface and front (Steps U1 and C1).
(2) Implementation of corresponding model generation tools (FE mesh generation schemes) to discretize the geometrical models into FE models (Steps U2 and C2).
(3) Verification and amendments (Step C3 and U3) of the geometrical and the FE models developed by checking the modelling results against experimental measurements.

In Steps C2 and U2, well defined mathematical descriptions of the modelled joints are essential. The main reason is that in order to study the general behaviour of the selected joint type, large parametric studies (Step U4 and C4) comprise a large numbers of FE models to cover the ranges of geometrical parameters selected. Hence, in order to obtain reliable modelling results, rather than to define the geometry of the joints based on preferences and selections from an individual analyst, all the FE models *must* be created based on a common geometrical description. In addition, consistent modelling

assumptions should be used when developing both the uncracked and the cracked models so that the latter model can be considered as an extension of the former model. For the development of geometrical models for large parametric FE studies, it is necessary to implement automatic model (mesh) generation tools for fast model generation so that the parametric study can be completed in a reasonable time. For the modelling of a cracked joint, similar to the experimental component, an optional step (Step C5) could be carried out for the modelling of ultimate failure strength and failure mode of the cracked joint (Lie et al. 2006b, 2006c, 2007).

Upon completion of the experimental and numerical studies, the development steps (Steps D1 to D4) follow to conclude the results and to deliver the following design aids to the user:

(1) Prediction tools of SCF and HSS values under different loading conditions.
(2) A prediction tool of the SIF values for surface cracks.
(3) Computation procedures for residual fatigue life of a cracked joint
(4) Failure assessment for the cracked joint.

One remark on the experimental and the numerical components is that they should not be treated as two separate and independent parts of the study. As shown in Figs. 1 and 2, they are highly coupled and they complement each another. Without the experimental investigation component, it is unlikely that reliable numerical models can be constructed and their predictions verified. On the other hand, without the numerical modelling component, planning for the experimental studies shall become a trial and error process and it shall be much harder to design a series of tests to obtain useful responses.

3. Joint type studies and tools developed

3.1 Joint type studies and scope of works

Table 1 lists the research projects conducted in a chronological order from 1998 to 2008. Joints made up of different section types (RHS and CHS) and configurations (T/Y/K) were tested. In Table 1, it can be seen that at least two full scale tests on both uncracked and cracked conditions were carried out in all projects. In addition, for the project RHS-T, the cracked joints were also re-configured for fracture and failure studies. The study period listed in Table 1 includes the time for both experimental and numerical studies, together with time spent to develop the modelling tools and to deliver the assessment methods. In general, it was found that the experimental component is the most expensive and time consuming part and accounted for about 75% of the project expenditures and 50% of the project time. A summary of the projects is tabulated in chronological order to show the increasing complexity of the joint type studied and the overlapping of the study periods between different projects. Such a project schedule was designed to optimize the use of the test rig so that by the time

when the experimental component of one project was finished, the test rig can be continuously used for the next project. Finally, it should be noted that due to the constraints imposed by the orange rig, all the studies only involved planar joints.

3.2 Tools and procedures developed

The tools and procedures developed can be classified into two distinctive sets. The first set consists of tools for the modelling of uncracked and cracked joints. The second set consists of procedures for the fatigue assessments of uncracked and cracked joints.

Tools for modelling of tubular joints

(1) A consistent geometrical modelling procedure for the weld

As the weld quality critically affects the fatigue performance of tubular joints (AWS 2008, API 2007), careful investigations were carried out to construct a realistic model for the weld profile along the tubular joint. The weld geometrical model developed (Lie et al. 2001) eventually served as the base for all numerical analyses with weld details. The model was constructed by considering the welding specifications from the design codes (AWS 2008, API 2007) in which the dihedral angle γ (Fig. 7a) is the main parameter that determines the minimum weld thickness, T_w at the chord face (Figs. 7c and 7d). The geometrical model developed defines T_w by considering the variation of γ at different points along the weld perimeter path. At any point T_w is equal to the sum of three thicknesses T_1, T_2 and T_3 (Figs. 7b – 7d) which account for the contact thickness based on pure geometrical intersection (T_1) and the effects of the weld fill in and cut out (T_2 and T_3) (Lie et al. 2003, 2006b, Chiew et al. 2004, 2007, Nguyen 2008). The final form of the model is refined and validated against many actual measurements. The objective of this modelling procedure is *not* to reproduce exactly the weld profiles created in actual joints. As it is well known that due to the nature of the fabrication process, it is impractical to assume that the final weld profile constructed will always satisfy precisely the pre-defined thickness requirement. In fact, it is found that for a carefully constructed joint, the actual weld thickness achieved is often greater than the minimum requirement. Hence, the present model developed is designed in such a way that weld thickness generated is (i) a continuous function along the whole intersection, (ii) satisfies the minimum requirements given by the design code and (iii) less than the thickness for most actual joints constructed.

(2) A consistent geometrical modelling procedure for the crack surface and front

The geometrical models for the crack surface and front (Lie et al. 2003, 2005a, 2006a, Lee et al. 2005) were developed based in the experimental measurements obtained from full scale tests (Chiew et al. 2004, 2007, Lie et al. 2006b). In the crack surface model, the crack surface is defined implicitly by considering its cross sections perpendicular to the tubular sections (Fig. 8a). After investigating the measurements obtained from full scale tests, it is found that the geometry of the crack surface can be defined conveniently by the angle ω as shown in Fig. 8a. In addition, ω can be considered as a constant for CHS joints (Lie et al. 2003, 2005a, Lee et al. 2005, Nguyen 2005) while it can be modelled as a linear function of the crack depth for RHS joints (Lee et al. 2007, 2009b). Once the crack surface is defined, the crack front can be constructed by measuring the relative positions of the two crack tips and the deepest point of the crack with respected to a fixed reference point on the section surface (Figs. 8b and 8c). The crack surface and front models are linked by a mapping procedure so that the crack front is described as a unsymmetrical bi-elliptical curve (Fig. 8b) on a projected plane. Such modelling procedure is again validated against all the experimental measurements obtained from the ACPD technique and is found to be reliable and gave good numerical modelling results.

(3) Standardized procedures for measuring the weld profile and crack surface shape

In order to gather information about the geometries of the weld profile and the crack surface from the test results and to validate the geometrical models developed, simple measurement procedures using clay moulding technique are developed. The common step of these procedures is to apply mouldable clay around the interested area and the moulding material is left to set (Fig. 9). The dried clay mould is then removed and measured to obtain the values of the desired parameters. For the measurement of the weld profile, a “slave” section is often employed to trace out the weld profile on a tracing paper which can then be digitized. For crack surface shape, a more complicated procedure is needed (Fig. 10). The cracked part is first cut out from the joint and opened up. Clay mould is applied to capture the shape of the crack surface which is then cut into sections for scanning and digital measurements. One advantage of these methods is that the clay mould is inexpensive to make and all measurement procedures are non-destructive so that repeated measurements could be applied to the specimen until successful measurements are obtained.

(4) A hierarchical mesh generation procedure for tubular joints

As large scale parametric study consists of thousands of analyses, it is infeasible to create FE meshes manually and the use of automatic mesh generation procedures is mandatory. Furthermore, as the

modelling of cracked joints is considered as the continuation of the modelling of uncracked joints, a *hierarchical* mesh generation procedure (Lee 2009b) was developed. This procedure allows a series of meshes with increasing levels of geometrical details to be created automatically. All the meshes in the series are consistent in the sense that all geometrical details included in the simpler meshes are inherited to the more complex meshes. An example of a partially overlapped CHS K-joint is shown in Figs. 11 and 12 to demonstrate the essential mesh generation steps. The simplest model and mesh created is a surface mesh (Fig. 11a) based in the geometrical intersection of the CHS sections. This surface mesh is generated by the general purpose mesh generation scheme developed by Lee (Lee 2003a, 2003b) and could be used for ultimate strength analysis. If detailed stress analysis is needed near the joint for fatigue assessment of uncracked joints, solid meshes with or without weld details (Fig. 11b and 11c) could be generated from the surface mesh by using a special thin-walled structure mesh generation scheme (Lee and Xu 2005) and a weld part generation procedure (Nguyen 2008). Finally, if cracked details are needed for the computation of SIF, an additional procedure (Nguyen 2008, Lee et al. 2009b) which extracts the crack affected zone (Fig. 12a) and creates the joint block (Fig. 12b) and the crack block (Figs. 12c and 12d) will be applied to the solid mesh. This automatic mesh generation procedure allows the modeller to create a large number of models in a short time for the parameter study and all the meshes generated are consistent regardless to the actual dimensions of the joints.

Procedures for fatigue assessments of tubular joints

(1) Interpolation technique for prediction of responses of tubular joints

In most design codes for tubular joints, the variations of key responses (e.g. SCF and SIF) with respect to the geometrical and loading parameters are described by some empirical equations. These equations are obtained by using multi-variable regression analysis based on the results obtained from numerical parametric studies. For simple joint types such as CHS T-joint under simple loading condition, these empirical equations are usually able to provide reasonable predictions. However, for the cases of a more complicate joint or a simple joint under complex loading, such an approach would often result in lengthy equations (Shao 2004). Furthermore, due to the complexity of the joint and the presence of many parameters, these lengthy equations would not be able to give good predictions over the whole range of parameters. To overcome this problem, a new approach was proposed (Shao 2004, Lie et al. 2005b, 2006d). The main concept of this new approach is that since the responses of the joints over the selected parametric ranges at some fixed intervals are computed during the parametric study, a logical way to approximate the variation of the responses can be obtained by using the standard Lagrangian

interpolation functions (Zienkiewicz et. al. 2005) that are frequently used in the FE analysis. Figure 13 shows an example where the variation of the response Φ is a function of a certain parameter ξ in the range [ξ_1, ξ_8]. The values of Φ at the nodes, ξ_i, i = 1,..,8 are already computed during the parametric study and are denoted as Φ_i. If the value of Φ at $\xi = \xi_{eval}$ is required, the third interval [ξ_3, ξ_4] that contains ξ_{eval} is first identified. The approximated value $\tilde{\Phi}(\xi_{eval})$ is then computed as

$$\tilde{\Phi}(\xi_{eval}) = L_1(\xi_{eval})\Phi_3 + L_2(\xi_{eval})\Phi_4 \tag{2}$$

In Eq. (1), $L_j(\xi)$, j=1, 2 are the first order Lagrangian interpolation function defined as

$$L_1(\xi) = \frac{\xi_{i+1} - \xi}{\xi_{i+1} - \xi_i}, \quad L_2(\xi) = \frac{\xi - \xi_i}{\xi_{i+1} - \xi_i}, i = 3 \tag{3}$$

For the 2D case, the variation of Φ is a function of two parameters ξ^1 and ξ^2 and the desired point ($\xi^1_{eval}, \xi^2_{eval}$) is enclosed by $2^2=4$ nodal points (Fig. 14). The i_1th interval along the ξ^1 axis and the i_2th interval along the ξ^2 axis that enclosing ($\xi^1_{eval}, \xi^2_{eval}$) can be easily identified. The approximated value $\tilde{\Phi}(\xi^1_{eval}, \xi^2_{eval})$ at the desired point can be obtained by extending Eqs. (1) and (2) as

$$\tilde{\Phi}(\xi^1_{eval}, \xi^2_{eval}) = \sum_{\alpha_1,\alpha_2=1,2}^{\alpha_1+\alpha_2 \le 4} L^1_{\alpha_1}(\xi^1_{eval}) L^2_{\alpha_2}(\xi^2_{eval}) \Phi_{i_1+\alpha_1-1, i_2+\alpha_2-1} \tag{4}$$

where

$$L^k_1(\xi^k) = \frac{\xi^k_{i_k+1} - \xi^k}{\xi^k_{i_k+1} - \xi^k_{i_k}}, \quad L^k_2(\xi^k) = \frac{\xi^k - \xi^k_{i_k+1}}{\xi^k_{i_k+1} - \xi^k_{i_k}}, k = 1,2 \tag{5}$$

In general, such an interpolation approach could be extended to the M-dimensional space involving a set of M parameters ξ^k, k=1,….,M. In this case, the desired point of evaluation $\boldsymbol{\xi}_{eval}$=($\xi^1_{eval}, \xi^2_{eval}, ..., \xi^M_{eval}$) is enclosed by a hypercube with 2^M nodes and M intervals [$\xi^k_{i_k}, \xi^k_{i_{k+1}}$] such that $\xi^k_{i_k} \le \xi^k_{eval} \le \xi^k_{i_{k+1}}$ for k=1,….,M. The expression of the approximated value at $\boldsymbol{\xi}_{eval}$, $\tilde{\Phi}(\boldsymbol{\xi}_{eval})$, is given by

$$\tilde{\Phi}(\boldsymbol{\xi}_{eval}) = \sum_{\alpha_k=1,2,k=1,..M}^{\sum \alpha_k \le 2M} \left(\prod_{k=1}^{M} L^k_{\alpha_k}(\xi^k_{eval}) \right) \Phi_{\boldsymbol{i_k}+\boldsymbol{\alpha_k}-1} \tag{6}$$

In Eq. (6), $\Phi_{\boldsymbol{i_k}+\boldsymbol{\alpha_k}-1}$ denotes the known nodal value of Φ at the node ($\xi^1_{i_1+\alpha_1-1}, \xi^2_{i_2+\alpha_2-1}, ..., \xi^k_{i_M+\alpha_M-1}$).

In an extensive numerical study carried out to access the performance of the above interpolation approach for the prediction of the SIF at the deepest point of surface cracks for gap CHS K-joints (Shao 2004), it was found that this approach could lead to more accurate and reliable response predictions with a lower relative error and a smaller error range (Fig. 15). In addition, by using this method, it is possible to estimate the upper error bound of the predicted responses and allows the user to obtain conservative response estimations during design.

(2) A procedure for the residual fatigue life prediction for cracked joints

With the geometrical models and the automatic mesh generation procedure, it is possible to estimate the residual fatigue life of a cracked joint. The starting point of this procedure is again the Paris Law (Eq. 1). After a series of FE models with different maximum crack depths are created and solved, the corresponding values of ΔK can be extracted from the modelling results. As C and m in Eq. (1) are independent of a, N *and* ΔK. Eq. (1) can now be integrated and the residual fatigue life of the cracked joint (normally defined as the number of loading cycles needed for the crack to penetrate through the affected section) can be computed as

$$\int dN = \int \frac{da}{C(\Delta K)^m} \tag{7}$$

As the values of ΔK for different values of a are available, Eq. (7) can be evaluated by using numerical integration so that the residual fatigue life, $N_{residual}$ for a cracked section with thickness t and current maximum crack depth a_c can be estimated as

$$N_{residual} = \int_{a_c}^{t} \frac{da}{C(\Delta K)^m} \approx \sum_{i=1}^{Q} w_i \left(\frac{1}{C(\Delta K_i)^m} \right) \tag{8}$$

where Q is the number of integration points (depths) used. w_i and ΔK_i are the weight and value of ΔK for the ith integration point, respectively. It is found that low (either first or second) order Newton-Cotes quadrature with Q = 10-15 is sufficient to evaluate Eq. (8) (Lee et. al. 2007, Nguyen 2008). Note that Eq. (8) is applicable to any joint type and it shows that estimation of residual fatigue life for a cracked joint is a computational intensive process as at least $Q \geq 10$ FE models are required to be created and solved before Eq. (8) can be evaluated.

4. Key research findings

4.1 Effects of weld details on SCF prediction

From the studies carried out to validate the correctness of the weld profile model, it is found that the weld thickness adopted in the numerical model can significantly affect the value of SCF computed. In addition, it was found that if no weld detail is included in the numerical model, this could result in a considerable overestimation of SCF. Figure 16 shows the variations of the SCF along the through brace of a partially overlapped K-joint (Nguyen 2008) predicted by using different weld profile models. The curves shown in Fig. 16 were obtained from 3D FE solid models and the quadratic extrapolation method for HSS calculation (Zhao et al. 2000, Wardenier 2002). It can be seen that while the numerical model constructed by using the actual measured weld thickness gave the best prediction within 5% error, the model without any weld detail overestimated the maximum SCF by 40% and is too conservative if used for fatigue assessment. While the actual weld profile gave the best prediction of SCF, it has no practical use in the design stage as the actual weld profile can only be obtained after the joint is constructed.

4.2 Effects of the angle parameter ω in SIF computation

After carried out many numerical experiments, it was found that the most critical geometrical parameter influencing the accuracy of the SIF prediction is the angle ω (Fig. 8a) that defines the shape of the crack surface. In general, a good SIF prediction could only be obtained when the difference between the value of ω adopted in the numerical model and the exact value is less than 10°. Detailed measurements conducted on cracked joints showed that for CHS joints, ω normally varies within the range of [0°-10°]. Hence, a constant value of ω = 0° could normally lead to good prediction of SIF for CHS joints. However, for RHS joints, ω could increase from 0° at the surface of the section to >75° when the crack depth approaches the thickness of the section (Chiew et al. 2007). This implies that a more complex geometrical model that allows for the variation of ω with respect to the crack depth (Lee et al. 2007) is needed for RHS joints. Figure 17 shows an example of the predicted SIF obtained by using different models of ω for a RHS joint (Lee et al. 2007). It shows that all models adopting a constant value of ω eventually leaded to poor predictions near the end of the fatigue life of the joint. The same figure also shows that a reasonably conservative prediction of SIF values could be obtained from a properly constructed surface model (Lee et al. 2007) in which the variation of ω is close to the actual value. Furthermore, the SIF values predicted from the proposed model are only slightly less

accurate than those obtained from the measured surface model which can only be constructed in an *ad hoc* manner after the cracked joint is opened and measured.

4.3 Accuracy of residual life estimation for cracked joints

Since Eq. (8) involves the integration of the term $1/(\Delta K)^m$, it is more difficult to predict the residual life of a cracked joint than the SIF as *all* the errors incurred during the estimation of the SIF shall accumulate and contribute to the total error of the residual life prediction. In practice, it is found that even with a fairly accurate estimation of the SIF (e.g. < 5%) over the entire crack growth history, the final error for the fatigue life prediction could be as high as 30%. Figure 18 shows an example that demonstrates such an error accumulation effect. It can be seen that even by adopting the measured surface model, it is difficult to achieve a 10% error in fatigue life prediction, especially during the initial phase of the crack growth when the crack depth is less than 15%-20% of the section thickness.

5. Conclusions and future studies

Presented in this paper is a summary of the research studies and findings on the fatigue performance of tubular joints obtained in the past ten years by the authors' research group at the Nanyang Technological University. Emphases are given to highlight the overall research methodology adopted. Both experimental study and numerical modelling are essential and they should complement each another in all stages of the study. This paper also summarizes the tools and procedures developed for fatigue performance assessments of uncracked and cracked joints. Finally, the key research findings discovered that are applicable to different tubular joint types are reported.

While it is demonstrated that the presented modelling procedures could lead to reasonable fatigue performance predictions for the joint types studied, there is certainly rooms for further research works and improvement. Some of the potential future research areas are listed below:

(1) More efficient procedure for residual fatigue life estimation

As mention in Section 3 residual fatigue life prediction is a computational expensive process. In case an urgent assessment for a cracked joint is required, a computationally less intensive procedure to evaluate Eq. (8) is needed. One possible approach to reduce the computational cost is to combine the interpolation approach with Eq. (8). Assumed that a parametric study on the variation of ΔK has been completed, the interpolation technique could then be employed to obtain the approximated values of ΔK_i without any additional FE analysis. However, from Section 4.3, this introduces an additional error

that could reduce the reliability of the predicted fatigue life. Thus, further research works are necessary to ensure that a reasonable conservative prediction could be obtained from such an approach.

(2) Studies on structural joints built from alternative materials

All the summaries, tools and procedures reported herein are developed for tubular joints constructed from hot rolled steel sections. Theoretically, all these works could be extended to tubular joints fabricated from other alternative materials such as high strength steel sections or cold formed steel hollow sections. In order to extend the presented methodology and tools for these materials, some fundamental studies on the basic fatigue behaviour for these alternative materials are needed.

(3) Improvement of modelling technique for a cracked joint

While the presented modelling procedures for cracked joints could lead to good SIF predictions for surface cracks with depths greater than 10% of the thickness of the section, it could not always lead to a good prediction for long and shallow cracks. Moreover, in order to obtain an accurate prediction of SIF, a large number of nodes and elements are required to capture the crack surface and crack mouth details. Hence, a possible direction of future research is to employ a more advanced modelling procedure such as the extended finite element method (Areias and Belytschko, 2005) to simplify the model generation process, to reduce the computational cost needed and to extend the range of application.

Acknowledgements

The financial support from the Ministry of Education, Singapore to carry out all the research projects listed in Table 1 is gratefully acknowledged. In addition, the authors would also like to thank their research students Dr. Huang Z. W., Dr. Wong S. M., Dr. Ji H. L., Dr. Yang Z. M., Dr. Shao Y. B., Ms. Nguyen, T. B. N. and Mr. Sopha T. for their help in conducting the research projects.

References

American Petroleum Institute (API), 2007. Recommended Practice for Planning, Designing and Constructing Fixed Offshore Platforms, API RP2A.

American Welding Society (AWS), 2008. ANSI/AWS D1.1/D1.1M-2008 Structural Welding Code-Steel, Miami, USA.

Areias, P. M. A. and Belytschko, T., 2005. Analysis of three-dimensional crack initiation and propagation using the extended finite element method. *International Journal for Numerical Methods in Engineering*, 63**,** 760-788.

Barsom, J. M. and Novak, S. R., 1977. Subcritical crack growth in steel bridge members, *NCHRP Report 181*, Transportation Research Board, National Research Council.

Chiew, S. P., Lie, S. T., Lee, C. K. and Huang Z.W., 2001. Stress intensity factors for a surface crack in a tubular T-joint, *International Journal of Pressure Vessels and Piping*, 78(10), 677 - 685.

Chiew, S. P., Lie, S. T., Lee, C. K. and Huang Z. W., 2004. Fatigue Performance of Cracked Tubular T Joints under Combined Loads. I: Experimental, *ASCE Journal of Structural Engineering,* 130(4), 562 - 571.

Chiew, S. P., Lee, C. K., Lie, S. T. and Ji H. L., 2007. Fatigue behaviors of Square-to-Square Hollow Section T-joint with corner crack. I: Experimental studies, *Engineering Fracture Mechanics*, 74(5), 703 – 720.

EN 1993, 2004a. *Eurocode 3: Design of steel structures, Parts 1.9 and 1.10*, CEN Central Secretariat, Rue de Stassart 36, B-1050 Brussels, BELGIUM.

Lee, C. K., 2003a. Automatic metric 3D surface mesh generation using subdivision surface geometrical model. Part 1: Construction of underlying geometrical model, *International Journal for Numerical Methods in Engineering*, 56(11), 1593 - 1614.

Lee, C. K., 2003b. Automatic metric 3D surface mesh generation using subdivision surface geometrical model. Part 2: Mesh generation algorithm and examples, *International Journal for Numerical Methods in Engineering*, 56(11), 1615 - 1646.

Lee, C. K., Lie, S. T., Chiew, S. P. and Shao, Y. B., 2005. Numerical models verification of cracked tubular T, Y and K-joints under combined loads, *Engineering Fracture Mechanics*, 72(7), 983 - 1009.

Lee, C. K. and Xu, Q. X., 2005. A new automatic adaptive 3D solid mesh generation scheme for thin-walled structures, *International Journal for Numerical Methods in Engineering*, 62(11), 1519 - 1558.

Lee, C. K., Chiew, S. P., Lie, S. T. and Ji, H. L., 2007. Fatigue behaviors of Square-to-Square Hollow Section T-joint with corner crack. II: Numerical Modelling, *Engineering Fracture Mechanics*, 74(5), 721 – 738.

Lee, C. K., Chiew, S. P., Lie, S. T., Sopha, T. and Nguyen, T. B. N., 2009a. Experimental studies on stress concentration factors for partially overlapped circular hollow section K-joint. To appear in *Advanced Steel Construction, an International Journal.*

Lee, C. K., Chiew, S. P., Lie, S. T. and Nguyen, T. B. N., 2009b. Adaptive mesh generation procedures for thin-walled tubular structures. To appear in *Finite Elements in Analysis and Design*.

Lie, S. T., Lee, C. K. and Wong, S. M., 2001. Modelling and mesh generation of weld profile in tubular Y-joint, *Journal of Constructional Steel Research*, 57(5), 467 - 580.

Lie, S. T., Lee, C. K. and Wong, S. M., 2003. Model and mesh generation of cracked tubular Y-joints, *Engineering Fracture Mechanics*, 70(2), 161 - 184.

Lie, S. T., Chiew, S. P., Lee, C. K. and Huang, Z. W., 2004. Fatigue Performance of Cracked Tubular T Joints under Combined Loads. II: Numerical, *ASCE Journal of Structural Engineering*, 130(4), 572 - 581.

Lie, S. T., Lee, C. K., Chiew, S. P. and Shao, Y. B., 2005a. Mesh modelling of cracked uni-planar tubular K-joints, *Journal of Constructional Steel Research*, 61(2), 235 - 264.

Lie, S. T., Lee, C. K., Chiew, S. P. and Shao, Y. B., 2005b. Validation of surface crack stress intensity factors of a tubular K-joint, *International Journal of Pressure Vessels and Piping*, 82(8), 610 - 617.

Lie, S. T., Lee, C. K., Chiew, S. P. and Yang, Z. M., 2006a. A consistent crack modelling and analysis of rectangular hollow section joints**,** *Finite Elements in Analysis and Design*, 42(8-9), 639-649.

Lie, S. T., Chiew, S. P., Lee, C. K. and Yang, Z. M., 2006b. Static strength of cracked square hollow section T joints under axial loads: I Experimental, *ASCE Journal of Structural Engineering,* 132(3), 368 - 377.

Lie, S. T., Lee, C. K., Chiew, S. P. and Yang, Z. M., 2006c. Static strength of cracked square hollow section T joints under axial loads: II Numerical, *ASCE Journal of Structural Engineering,* 132(3), 378 - 386.

Lie, S. T., Shao, Y. B., Lee, C. K. and Chiew, S. P., 2006d. Stress intensity factor solutions for semi-elliptical weld-toe cracks in tubular K-joints, *Advances In Structural Engineering,* 9(1), 129-139.

Lie, S. T., Yang, Z. M. Chiew, S. P. and Lee, C. K., 2007. The ultimate behaviour of cracked square hollow section T-joints, *Advanced Steel Construction, an International Journal,* 3(1), 443-458.

Nguyen, T. B. N., 2008. Model and mesh generation of partially overlapped circular hollow section k-joints for fatigue studies. *Ph.D. Thesis*, School of Civil and Environmental Engineering, Nanyang Technological University, Singapore.

Paris, P. and Erdogan, F., 1963. A critical analysis of crack propagation laws, Journal of Basic Engineering. *Transactions of the American Society of Mechanical Engineers* December, 528-534.

Technical Software Consultant Ltd., 1991. ACFM Crack Microgauge – Model U10 User Manual. Milton Keynes, UK: The Open University.

Shao, Y. B., 2004. Fatigue behaviour of uniplanar CHS gap K-joints under axial and in-plane bending loads, *Ph.D. Thesis*, School of Civil and Environmental Engineering, Nanyang Technological University, Singapore.

Sopha, T., Nguyen, T. B. N., Chiew, S. P., Lee, C. K. and Lie, S. T., 2008, Stress analysis and fatigue test on partially overlapped CHS K-joints, *Advanced Steel Construction, an International Journal,* 4(2), 134-146.

Wardenier J., 2002. *Hollow Sections in Structural Applications*, Bouwen met Staal, Rotterdam, Netherlands.

Zhao, X.L., Herion, S., Packer, J.A., Puthli, R., Sedlacek, G., Wardenier, J., Weynand, K.,van Wingerde, A. and Yeomans, N., 2000. Design Guide for Circular and Rectangular hollow Section Joints under Fatigue Loading. CIDECT, TUV Germany.

Zienkiewicz, O. C., Taylor, R. L. and Zhu, J. Z, 2005. *The Finite Element Method: Its Basis and Fundamentals.* Sixth Edition, Elsevier Butterworth-Heinemann, UK.

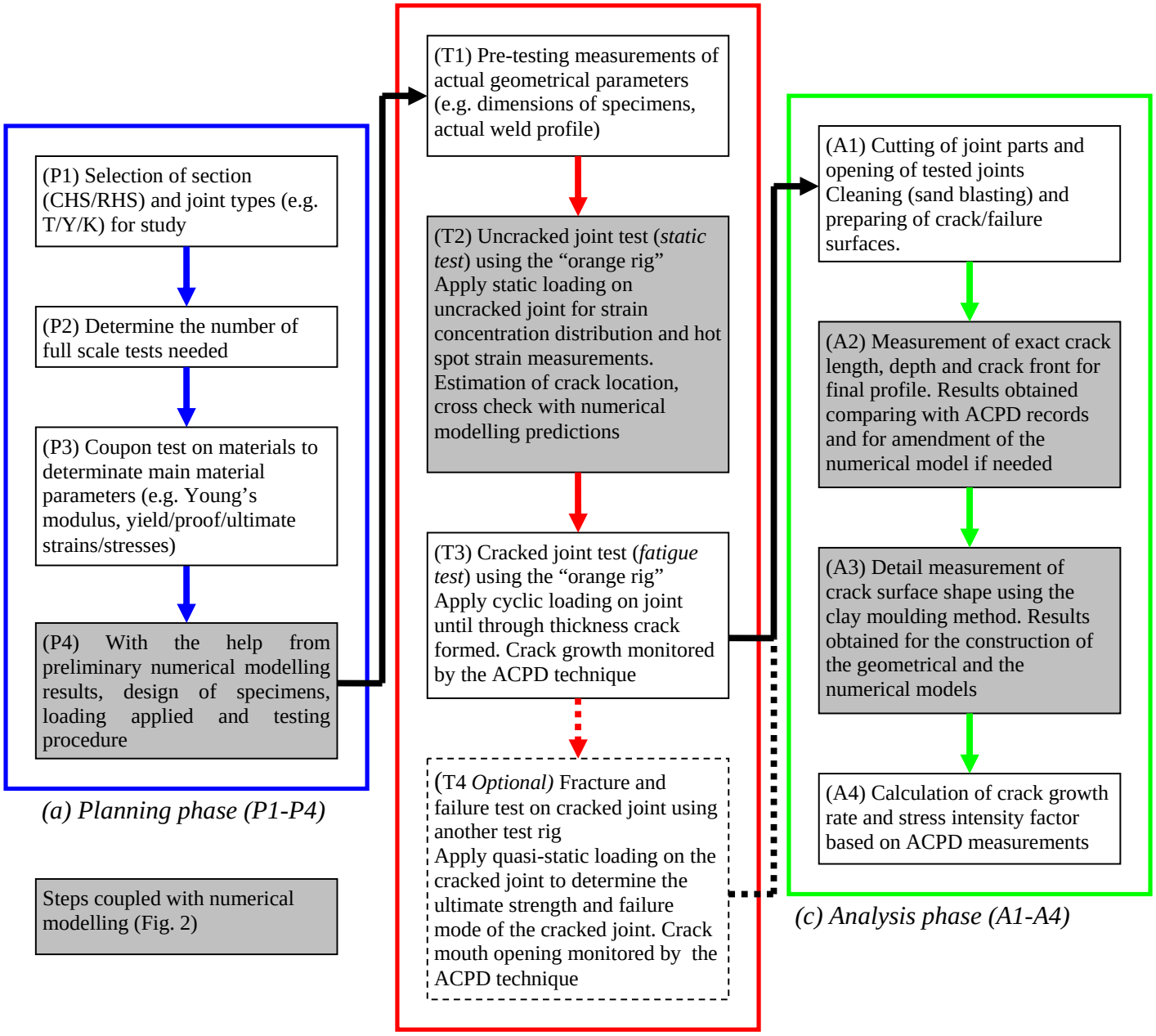

Figure 1. An overall flow chart for the experimental component

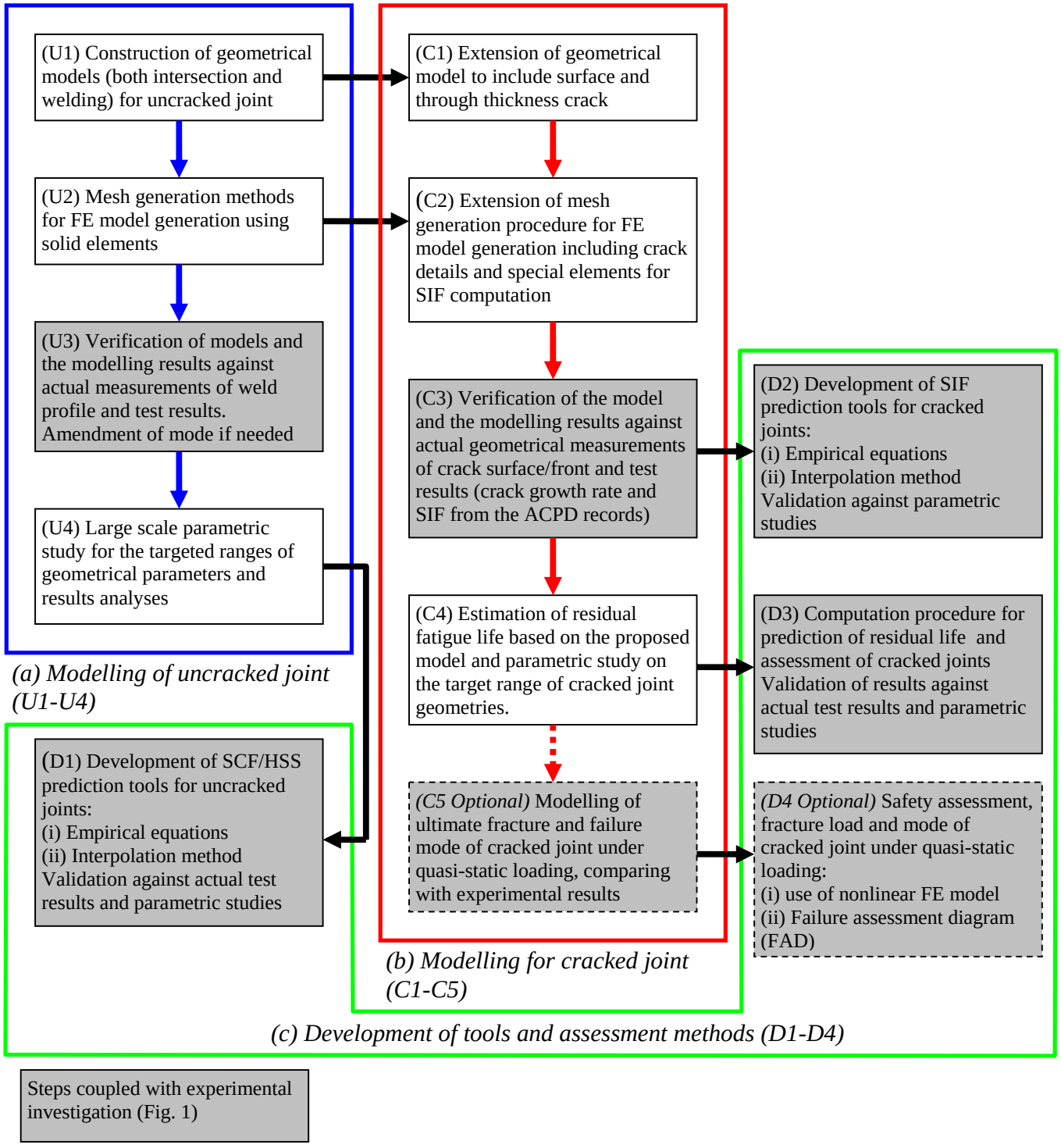

Figure 2. An overall flow chart for the numerical component

Figure 3. The 25-tonne multi-axis dynamic testing frame (the “Orange Rig”) for fatigue testing

Figure 4. Typical set up of strain gauges during static test

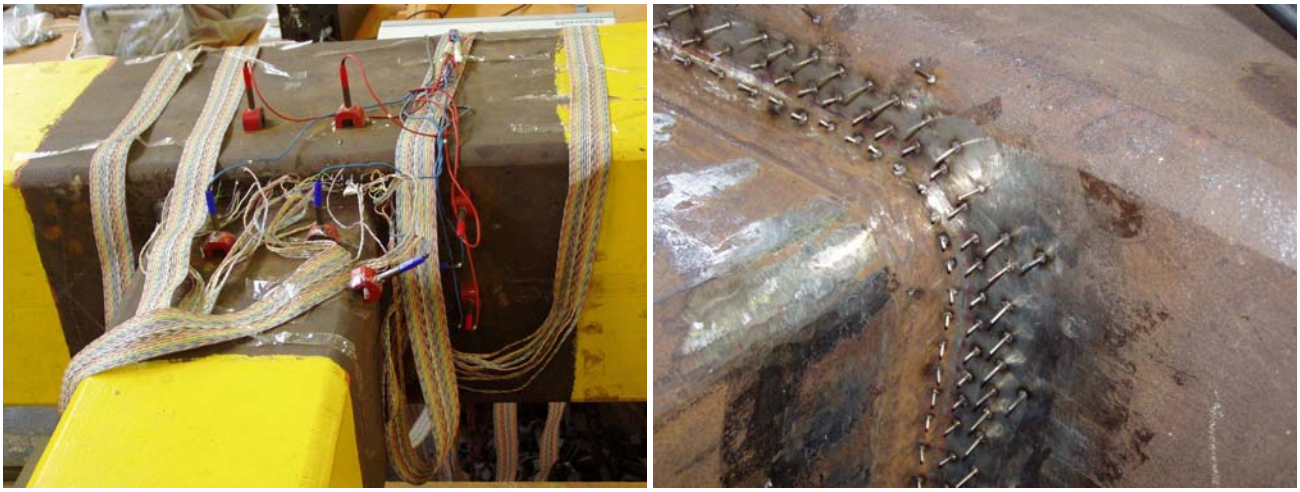

(a) Set up of ACPD during testing (b) ACPD probes attached to specimens

Figure 5. Typical set up of ACPD equipment for crack monitoring during fatigue test

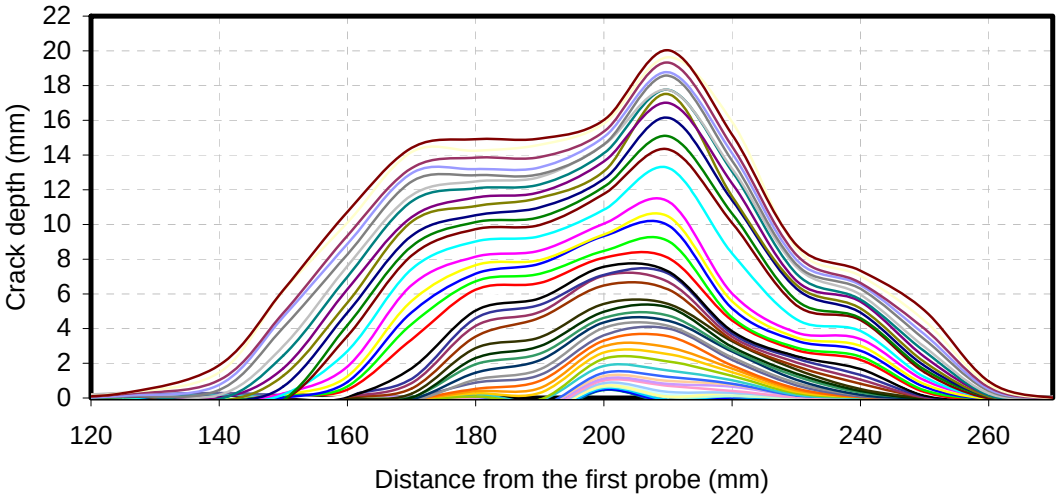

Figure 6. Typical crack profile recorded by using ACPD technique
(each line corresponding to 1000 cycles of cyclic loading)

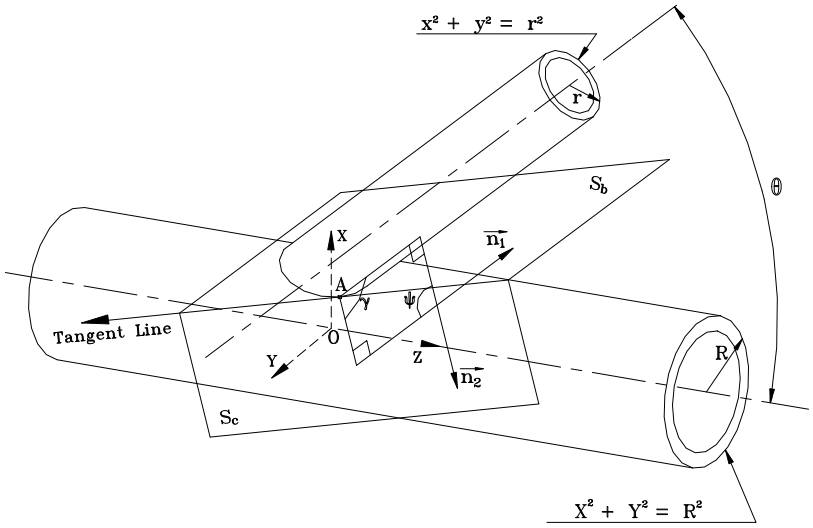

(a) Definition of dihedral angle for a CHS joint

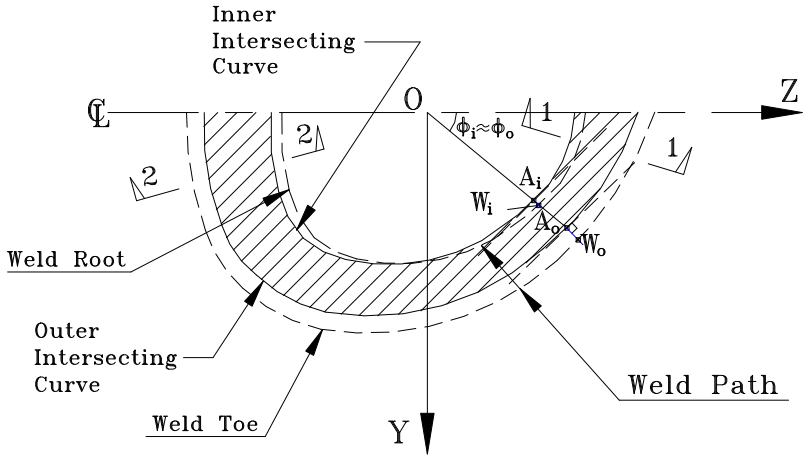

(b) Weld profile of the joint (plan view)

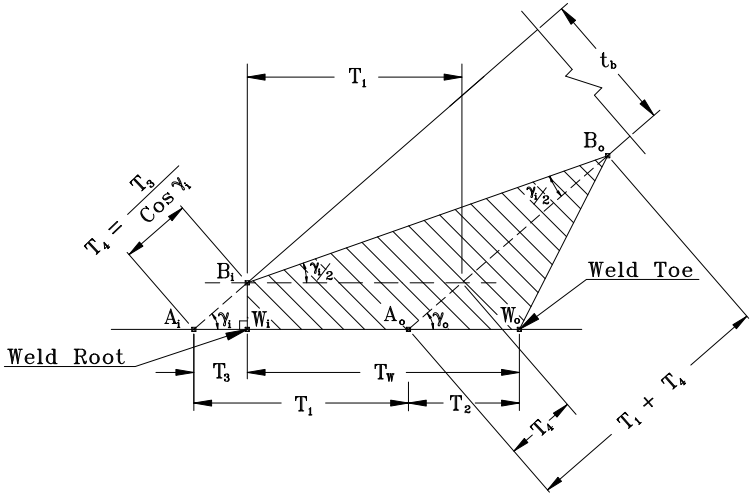

(c) Section view for section 1-1: (30° ≤ γ < 90°)

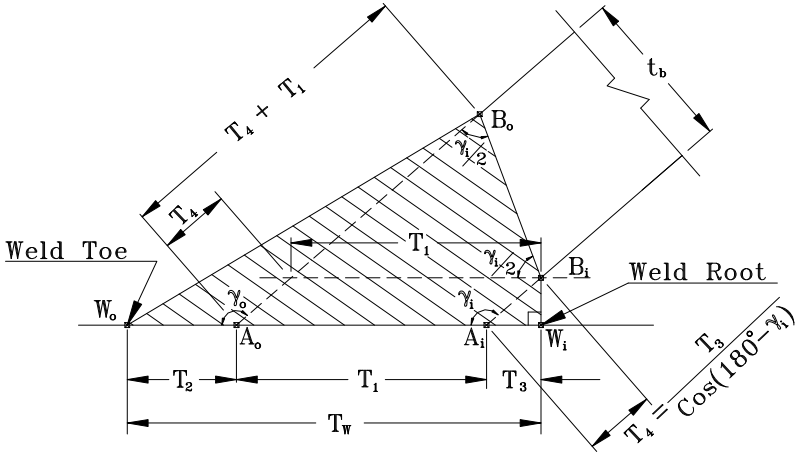

(d) Section view for Section 2-2: (90° ≤ γ < 180°)

Figure 7. Geometrical model for the welding of CHS tubular joints

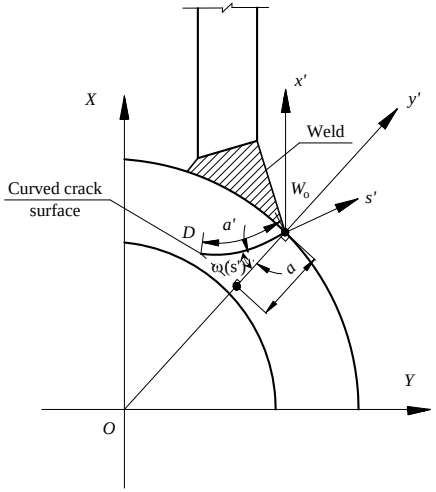

(a) Crack surface and the driving angle ω

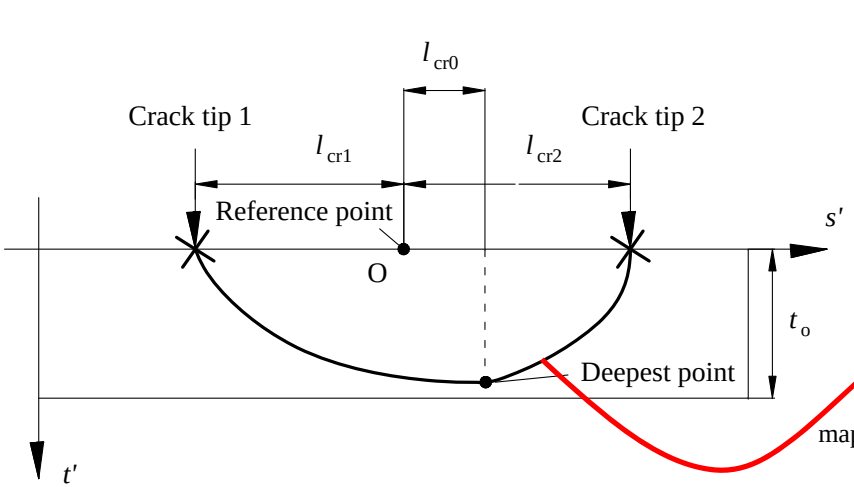

(b) Definition of the crack front in the parametric space

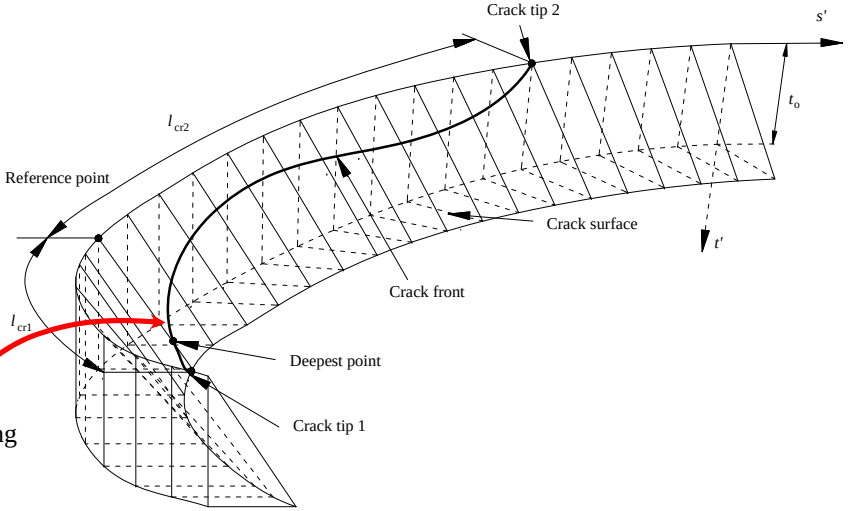

mapping

(c) Mapping to physical crack surface

Figure 8: Geometrical models for the crack surface and front

(a) Applied wet, soft clay along joint

(b) Removal of dried clay

(c) Weld profile printed on clay

(d) Weld profile traced out using a “slave” section

Figure 9. A simple procedure for weld profile measurement

(a) Opening of cracked joint

(b) Cutting out of cracked part

(c) Apply clay mould

(d) Removal and marking on clay mould

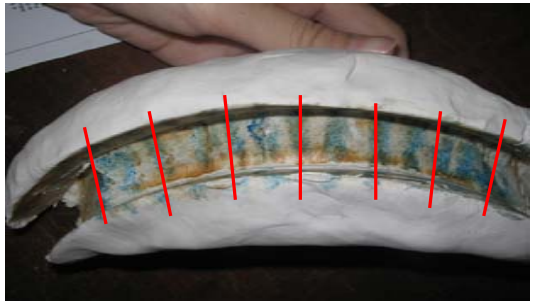

(e) Define different sections for surface

(f) Cut clay mould in sections

(g) Section ready for scanning

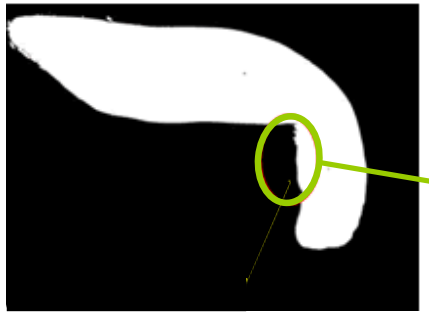

(h) Scanned section into CAD software

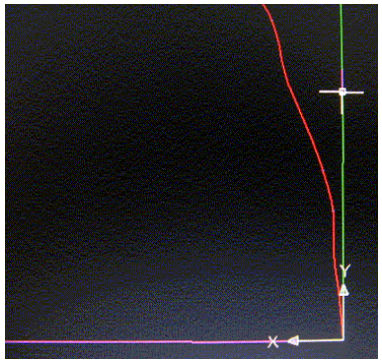

(i) Measurement of surface profile digitally

Figure 10. A simple procedure for measurement of crack surface and front shapes

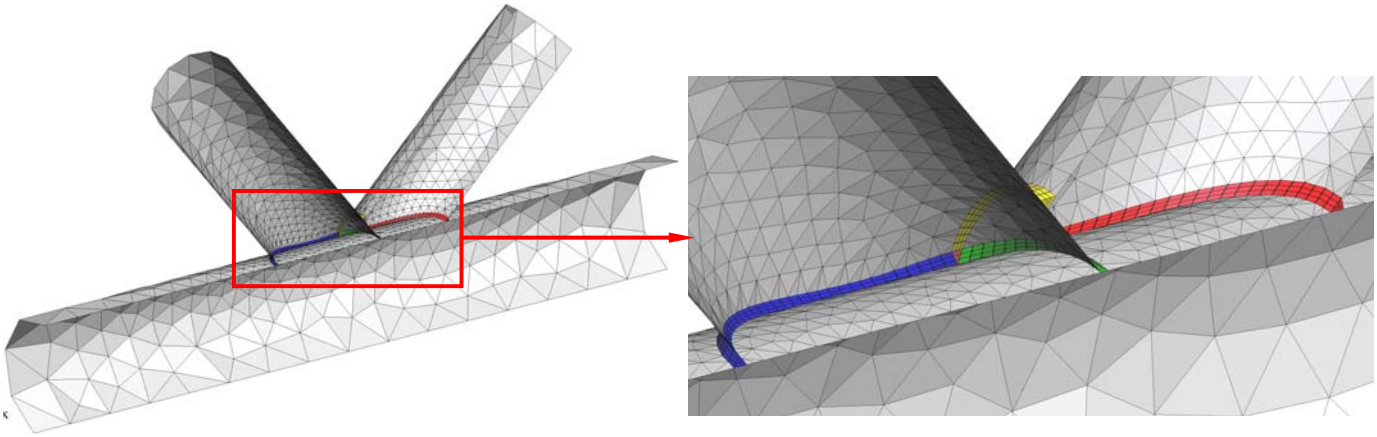

(a) Surface mesh with weld details

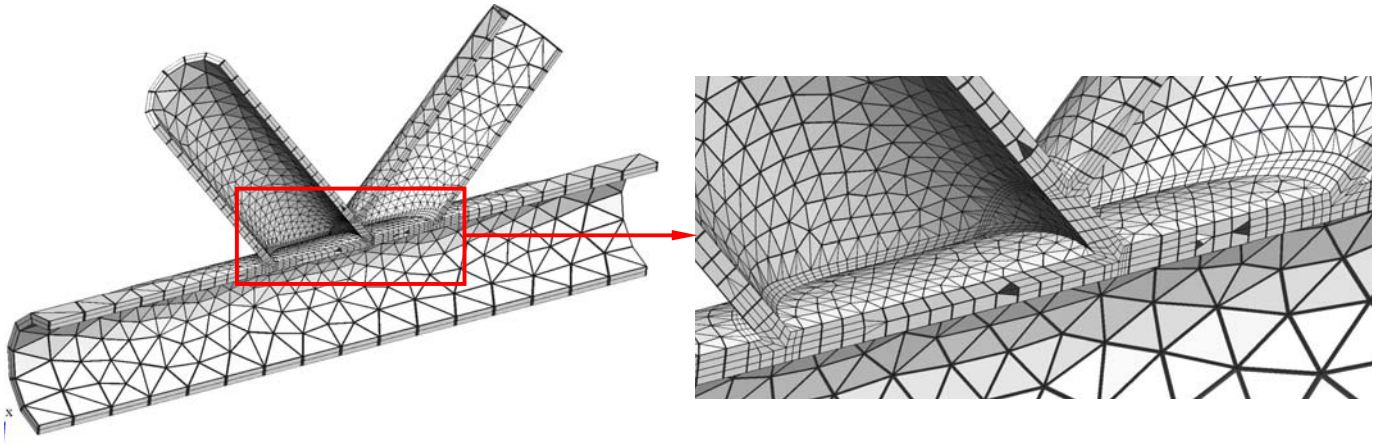

(b) Solid mesh without weld details

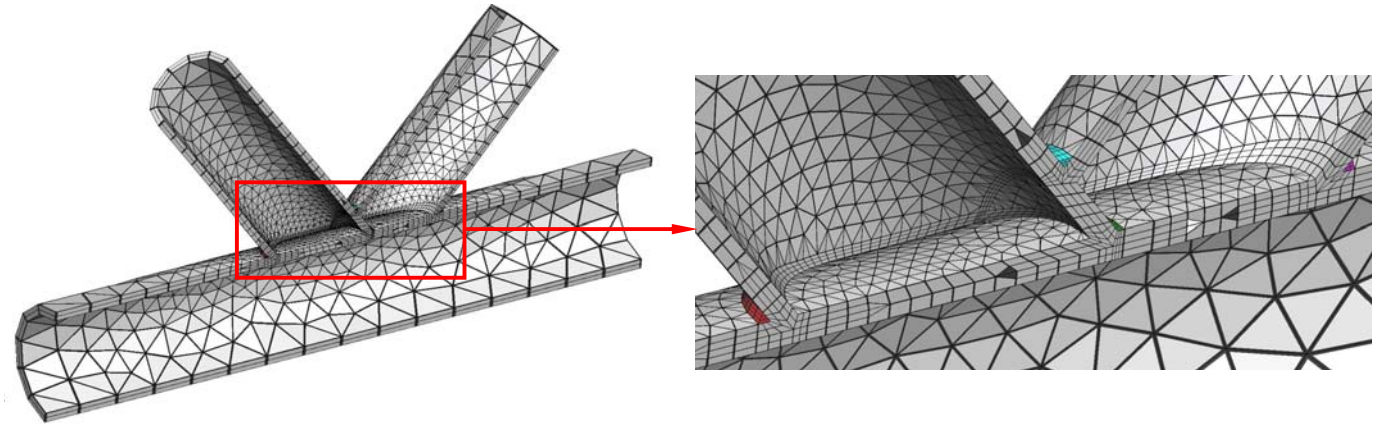

(c) Solid mesh with weld details

Figure 11. Mesh generation schemes for uncracked joint

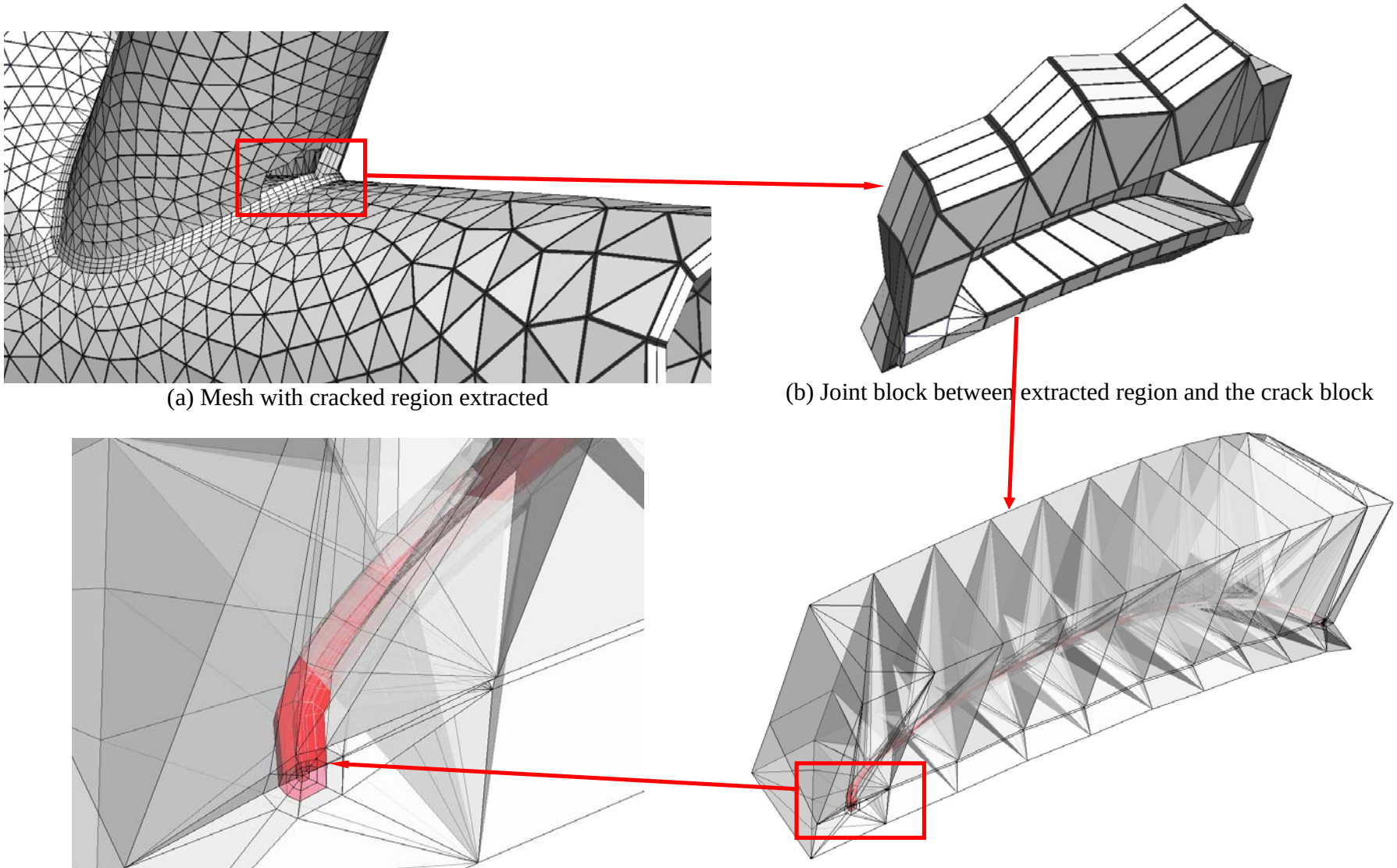

(a) Mesh with cracked region extracted

(b) Joint block between extracted region and the crack block

(c) Mesh for the crack block

(d) Zoom in view near crack mouth

Figure 12. Mesh generation for cracked joint

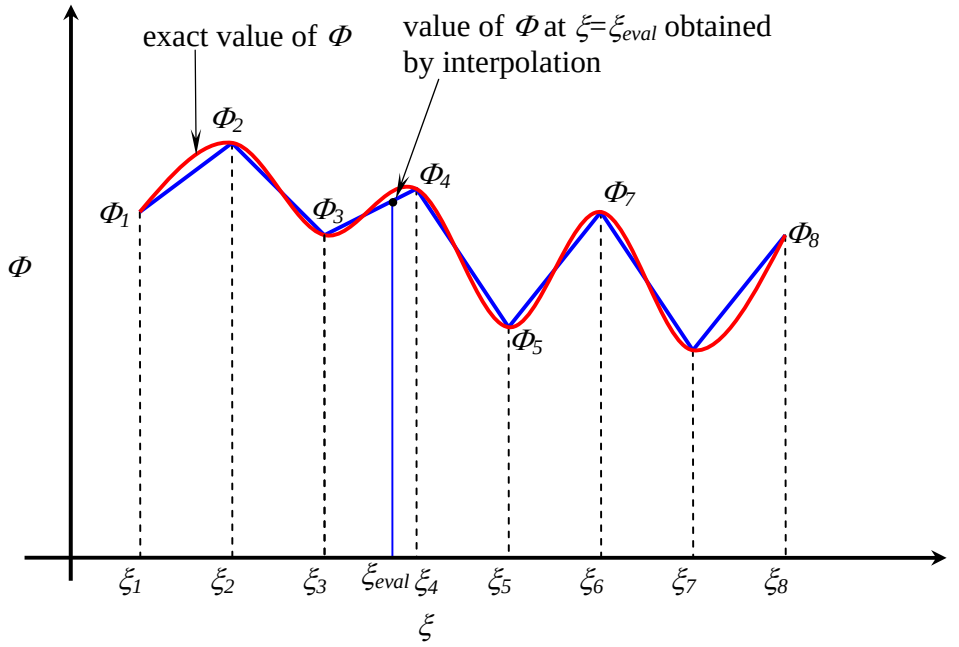

Figure 13. Computation of Φ by the interpolation method for the single parameter (1D) case

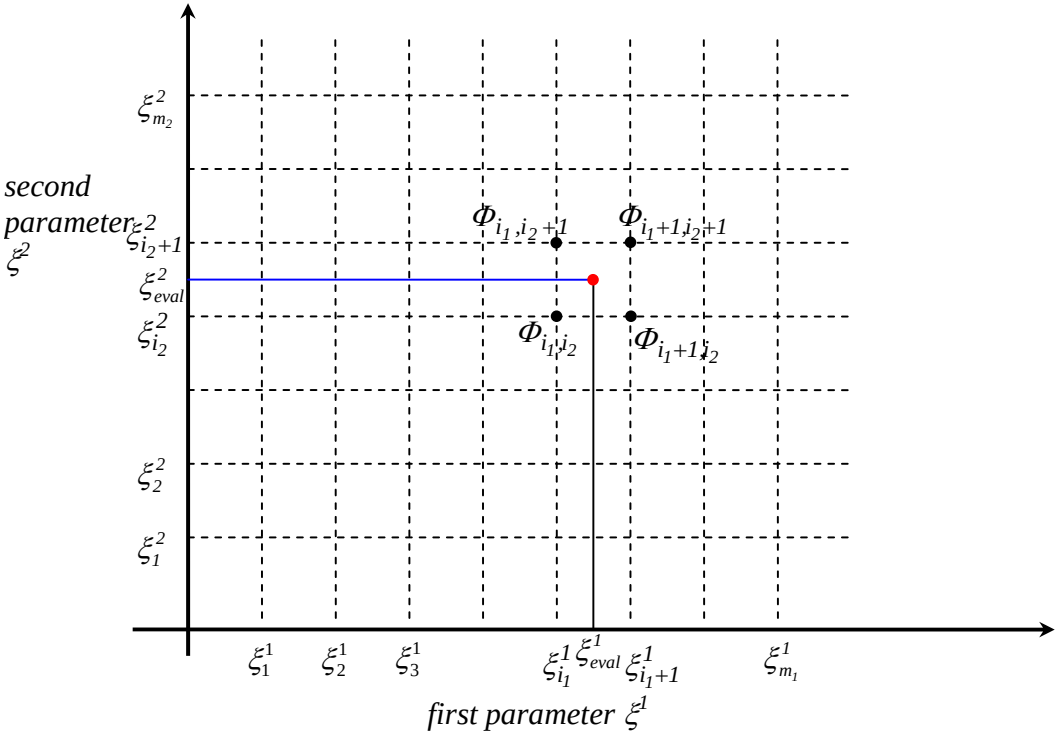

Figure 14. Computation of Φ by the interpolation method for the two parameters (2D) case

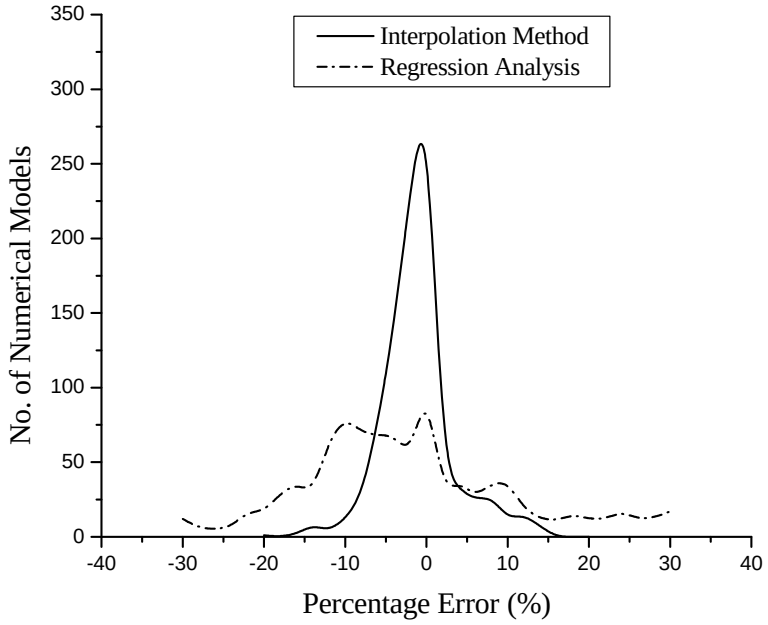

Figure 15. Comparison of error distribution between estimated responses obtained from the interpolation method and regression analysis

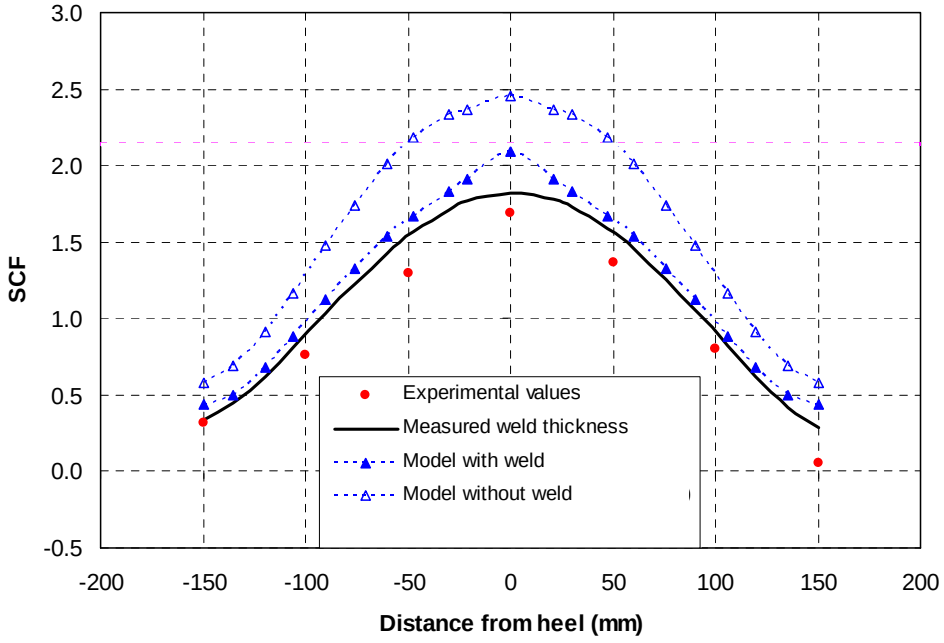

Figure 16. Effect of weld details on the modelling results for a partial overlapped K-joint: A plot of the through brace SCF variation under in-plane bending

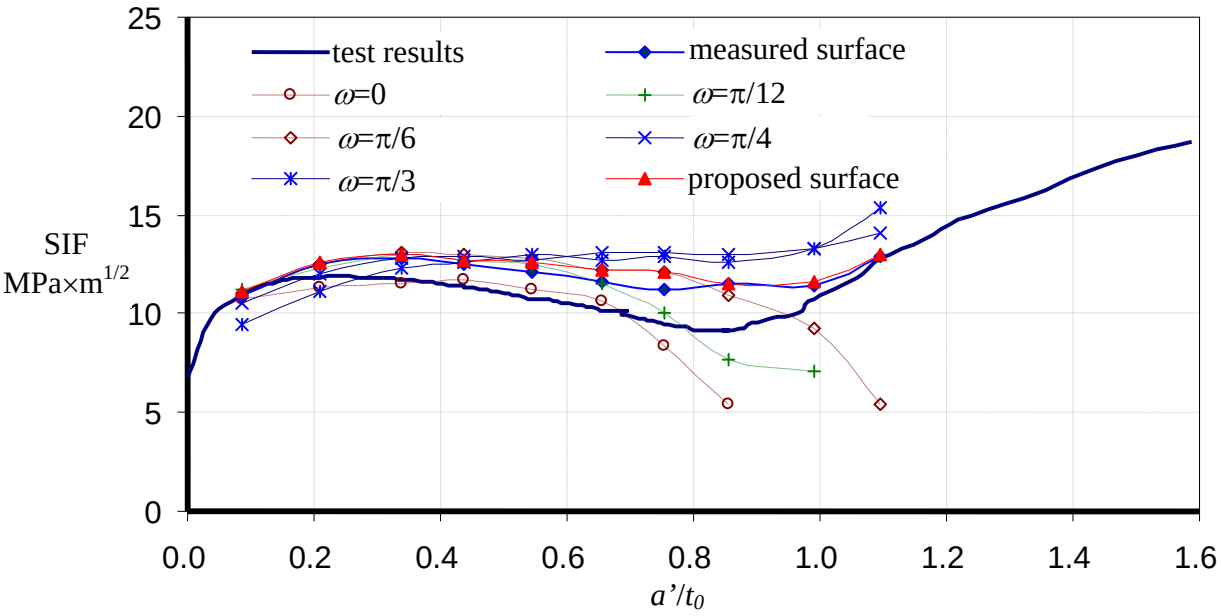

Figure 17. Predictions of SIF at the deepest point for a square-to-square RHS joint using different models of ω (a' = depth of the surface crack, Figure 8a, t_0 = thickness of section)

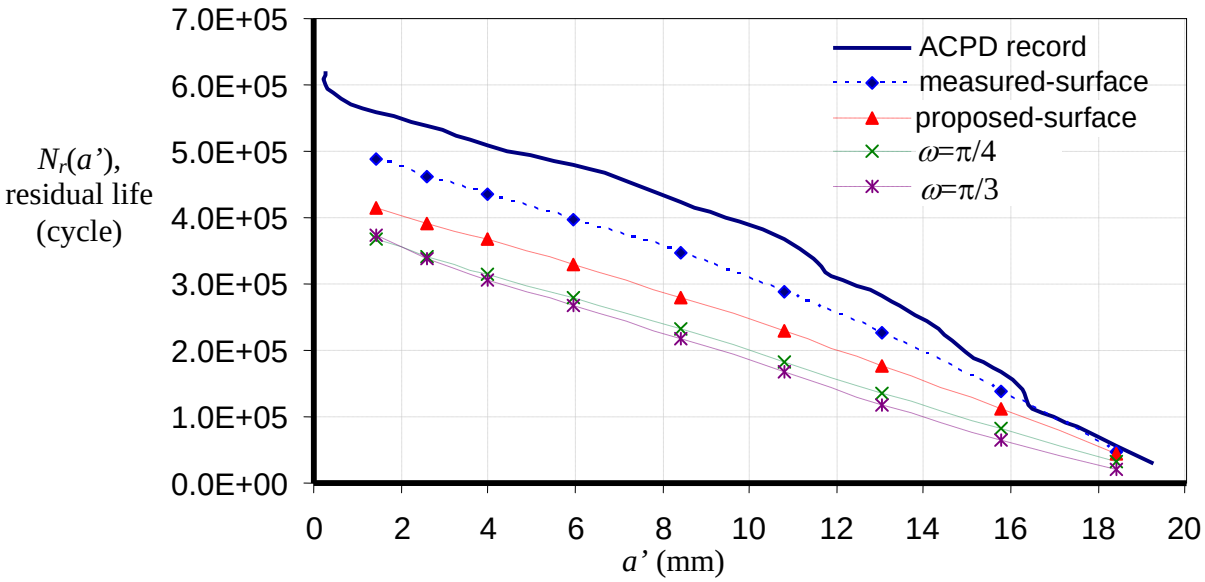

Figure 18. Prediction of residual fatigue life using different models of ω shown in Figure 17 (a' = depth of the surface crack, Figure 8a, t_0 = thickness of section)

Table 1 A summary on the projects completed and scope of works

Project name	**Period of study**	**Section Type**	**Joint configuration**	**Number of full scale tests**	**Scope of work**	**Reference**
CHS-T	1998-2002	CHS	T joint	3	uncracked and cracked fatigue analysis	Chiew et. al 2001, 2004 Lie et al. 2003, 2004
CHS-GK	2000-2004	CHS	Gapped K joint	2	uncracked and cracked fatigue analysis	Lee et al. 2005 Lie et al. 2005a, 2005b, 2006d
RHS-T	2002-2006	RHS	T joint	4	uncracked and cracked fatigue analysis Fracture and failure for cracked joint	Chiew et al. 2007 Lee et al. 2007 Lie et al. 2006a, 2006b, 2006c. 2007
CHS-LK	2004-2008	CHS	Partially overlapped K joint	3	uncracked and cracked fatigue analysis	Lee and Xu 2005 Lee et al. 2009a, 2009b Sopha et al. 2008